INSTRUMENTS AND TECHNIQUES

J. R. P. Geiger · J. Bischofberger · I. Vida · U. Fröbe
S. Pfitzinger · H. J. Weber · K. Haverkampf · P. Jonas

Patch-clamp recording in brain slices with improved slicer technology

Abstract The use of advanced patch-clamp recording techniques in brain slices, such as simultaneous recording from multiple neurons and recording from dendrites or presynaptic terminals, demands slices of the highest quality. In this context the mechanics of the tissue slicer are an important factor. Ideally, a tissue slicer should generate large-amplitude and high-frequency movements of the cutting blade in a horizontal axis, with minimal vibrations in the vertical axis. We developed a vibroslicer that fulfils these in part conflicting requirements. The oscillator is a permanent-magnet-coil-leaf-spring system. Using an auto-resonant mechano-electrical feedback circuit, large horizontal oscillations (up to 3 mm peak-to-peak) with high frequency ($\approx$90 Hz) are generated. To minimize vertical vibrations, an adjustment mechanism was employed that allowed alignment of the cutting edge of the blade with the major axis of the oscillation. A vibroprobe device was used to monitor vertical vibrations during adjustment. The system is based on the shading of the light path between a light-emitting diode (LED) and a photodiode. Vibroprobe monitoring revealed that the vibroslicer, after appropriate adjustment, generated vertical vibrations of <1 μm, significantly less than many commercial tissue slicers. Light- and electron-microscopic analysis of surface layers of slices cut with the vibroslicer showed that cellular elements, dendritic processes and presynaptic terminals are well preserved under these conditions, as required for patch-clamp recording from these structures.

Introduction

Patch-clamp recording from neurons has advanced our understanding of electrical and chemical signalling in the mammalian central nervous system substantially. Landmarks of technical improvement were the application of patch-clamp techniques to neurons in brain slices [2, 5], the combination with infrared differential interference contrast (IR-DIC) videomicroscopy [4, 13, 19, 21], the recording from pairs of synaptically connected neurons [9, 12, 14, 16] and the recording from small subcellular structures, such as dendrites and presynaptic elements [3, 6, 8, 15, 19, 20, 21]. For both paired recording and recording from subcellular structures, the quality of the slice preparation is of eminent importance. When recordings are made under the visual control provided by IR-DIC [19, 21], the integrity of the superficial layers of the slice is a particularly relevant issue. As structures are approached typically with positive pressure in the patch pipette without "cleaning" [19, 21], recording is restricted to a region 10–100 μm below the surface of the slice. Unfortunately, however, the preservation of the superficial layers is often poor with conventional slicing techniques [7, 17].

Several factors are thought to affect slice quality. First, solutions used for cutting and storage are important. For example, addition of ascorbic acid [3, 18] or pyruvate [3, 6] and replacement of NaCl by sucrose [8] are thought to be advantageous for the preservation of the tissue. Second, the properties of the tissue slicer used for cutting are important. Experience shows that three aspects are of primary relevance: (1) the amplitude of the horizontal oscillation has to be sufficiently large, especially for brain regions with a high abundance of myelinated fibres (such as spinal cord or brainstem); (2) the fre-

J.R.P. Geiger · J. Bischofberger · U. Fröbe · S. Pfitzinger
H.J. Weber · K. Haverkampf · P. Jonas (✉)
Physiologisches Institut der Universität Freiburg, Abteilung I,
Hermann-Herder-Strasse 7, 79104 Freiburg, Germany
e-mail: jonasp@uni-freiburg.de
Tel.: +49-761-2035150, Fax: +49-761-2035204

I. Vida
Anatomisches Institut der Universität Freiburg, Abteilung I,
Albertstrasse 17, 79104 Freiburg, Germany

quency of the horizontal oscillation has to be sufficiently high to minimize countermovements of the tissue block; (3) the amplitude of possible vertical vibrations of the cutting blade must be minimal, to avoid compression of the superficial layers of the tissue.

Several different constructions of tissue slicers are available commercially, which are based on either motor/ex-centre designs or on iron core/magnetic-coil systems. Unfortunately, however, these commercial slicers do not fulfil the requirements of large amplitude and high frequency at the same time. Furthermore, the amplitude of possible vertical vibrations of the cutting blade generated by these slicers is unknown. In this paper, we report techniques for maximizing both amplitude and frequency of the horizontal oscillations of a slicer. In addition, we describe methods for measuring vertical vibrations and for minimize these using an adjustment mechanism. In combination, the techniques allowed us to cut slices with consistently well-preserved surface layers, as required for patch-clamp recording from presynaptic elements in the hippocampus [8]. Part of the work has been published in abstract form [10].

Materials, methods, and results

An adjustable magnet-coil-leaf-spring system driven by an auto-resonant feedback circuit

To generate large-amplitude, high-frequency oscillations confined to a horizontal axis, with minimal vibrations in the vertical axis, we developed a "vibroslicer" (Figs. 1, 2 and 3). The head of the slicer comprises a permanent magnet-coil-leaf-spring system. A pair of leaf springs holds the oscillating front piece laterally. The blade holder is adjustable, allowing alignment of the cutting edge of the blade with the major axis of the oscillation. Using a mechano-electrical feedback system, harmonic oscillations of constant amplitude are generated at the resonance frequency.

Construction details

The vibroslicer head is a permanent-magnet-coil-leaf-spring system (Fig. 1). The system contains two magnet blocks, one above and one below the magnetic coil. Each block comprises three magnets (neodymium, NdFeB, type Mq201105 N1; 20×10×5 mm; Dexter, Garching, Germany; magnetic remanence 1.1 T according to data sheets) and two pole shoes (S235J0 steel, material number 1.0114). Both blocks are screwed tightly to an aluminium front piece that is held by vertically oriented leaf springs on either side (spring thickness h 2 mm, spring width b 40 mm; X12CrNi177, material number 1.4310 spring steel). The system is relatively flexible against horizontal movements, but extremely stiff against vertical movements or torsion, which helps to minimize vibrations in the vertical axis.

The magnetic coil consists of 1,300 windings of insulated copper wire (wire diameter 0.35 mm; inductivity L 44.1 mH; ohmic resistance R 25 Ω). The coil is placed in the centre of the system and is screwed tightly to the aluminium head block. The vertical distance between the surface of the coil and the pole shoes is $\approx$0.5 mm.

Current flow through the windings of the coil generates a Lorentz force perpendicular to the directions of both magnetic field and current flow (Fig. 1A). As the coil is fixed, this is translated into horizontal movement of the front piece. The permanent-magnet-coil system is very powerful; the force generated is $\approx$30 N A^{-1} DC current. Furthermore, the system generates strictly horizontal forces, again helping to minimize vibrations in the vertical axis.

Adjustment of the head

To minimize vibrations in the vertical (top-bottom) axis, the edge of the cutting blade must be exactly parallel to the major axis of the oscillation of the front piece. To achieve this, an adjustment mechanism based on a differential thread screw (Fig. 1C) was employed. Turning the screw rotates the blade holder against the front piece around a horizontal (back-to-front) axis; a spring pulls the two parts together to minimize hysteresis. A vibroprobe device is used to achieve optimal positioning (see below). The optimal position is fixed by tightening a fixation screw (Fig. 1D, E).

An analogous adjustment option to minimize vibrations in the horizontal (back-front) axis may be also useful (not illustrated). To achieve this, a micrometer screw is mounted on one of the leaf springs, pressing against its rear side. After loosening the Allen screws fixing the leaf spring, it can be moved back and forth in a defined manner. A two-dimensional vibroprobe device is used to reach the optimal position (see below).

Auto-resonant feedback circuit

To obtain large horizontal oscillation amplitudes with minimal external forces, the system must be driven at the resonance frequency. To achieve this, a mechano-electrical feedback loop was employed (Fig. 2A). Two reflection light barriers (CNY70, Vishay Telefunken, Heilbronn, Germany) in the vibroslicer head, directed towards a lateral vibrating part on each side, measure the displacement of the front piece in real time. The output from the reflection light barriers is fed into a series of three operational amplifiers (OP1–OP3). OP1 and 3 have constant gain, OP2 has adjustable gain. OP3 is a power amplifier (OPA544, Burr-Brown, Tucson, Ariz., USA).

The oscillatory properties of the system can be understood in terms of linear basic element theory [1]. The magnetic coil represents a so called PT$_1$ element (proportional-time 1 i.e. 1st-order delay element, for which the phase shift ($\Delta\varphi$) between voltage and current, $\Delta\varphi_1$, is $\approx$0 for a small angular frequency ω and $\approx$–90$°$ for large ω, and for
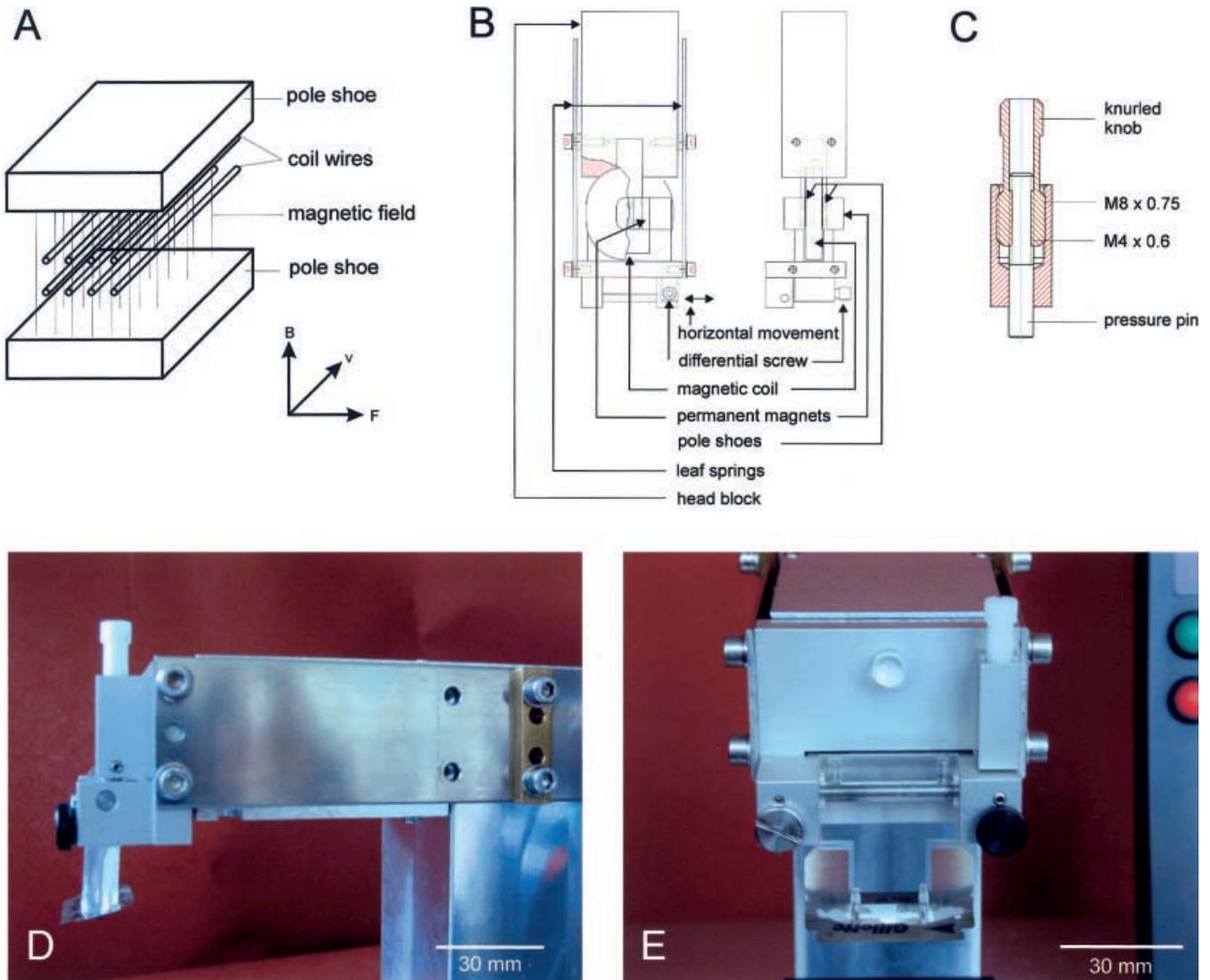
Fig. 1A–E Principle and mechanics of the vibroslicer head. **A** Principle of operation. A magnet coil is positioned between two permanent magnet arrays. *Upper* and *lower blocks*: pole shoes, *vertical thin lines*: magnetic field, *horizontal wires*: parts of the coil. The 3-D coordinates (*lower right*) indicate the directions of the magnetic field (*B*), the mean velocity of electrons (*v*) and the resulting Lorentz force (*F*). **B** Schematic drawing of the body of the vibroslicer head; view from the top (*left*) and from the side (*right*). **C** Differential thread screw system used to align the edge of the cutting blade with the major axis of the oscillation. The pitch of the *upper* and *lower* threads is 0.75 and 0.6 mm, respectively, which gives a difference of 0.15 mm/turn. **D**, **E** Photograph of the vibroslicer head, view from the side (**D**) and from the front (**E**). Note the axis for rotation (*left bottom* in **E**), the differential thread screw (*right* in **E**) and the fixation screw (*right bottom* in **E**) for adjustment. Also note the Perspex blade-holder with a mounted Gillette® razor blade. The blade holder has sharp edges (rather than flat surfaces) on either side, which is favourable from an hydrodynamic point of view after immersion in cutting solution

which the dependence of $\Delta\varphi_1$ on ω in the intermediate range of ω is roughly linear). The magnet-leaf-spring system represents a so called PT_2 element (proportional-time 2 i.e. 2nd-order delay element, for which $\Delta\varphi$ between force and elongation, $\Delta\varphi_2$, is ≈ 0 for small ω and $\approx -180°$ for large ω, and for which there is an extremely steep dependence of $\Delta\varphi_2$ on ω in a narrow band around the resonance point). All other elements in the loop are P (proportional) elements, implying that they generate 0° phase shift. At the resonance frequency, $\Delta\varphi_{total}=\Delta\varphi_1+\Delta\varphi_2\approx -180°$. If an inversion is introduced at one of the elements, a positive feedback loop is assembled and the system will oscillate.

In an ideal system, mechanical oscillations of constant amplitude could be generated by setting the total loop gain to 1. This is difficult to achieve in a real system, because even slight changes in load will lead to a situation where the oscillation amplitude decreases to zero (or increases to maximal possible values). To generate an oscillation with a constant amplitude, automatic gain control is required. This was implemented as follows. OP1 gives a voltage signal proportional to the mechanical amplitude. The signal is rectified and filtered (filter time constant ≈ 30 ms).
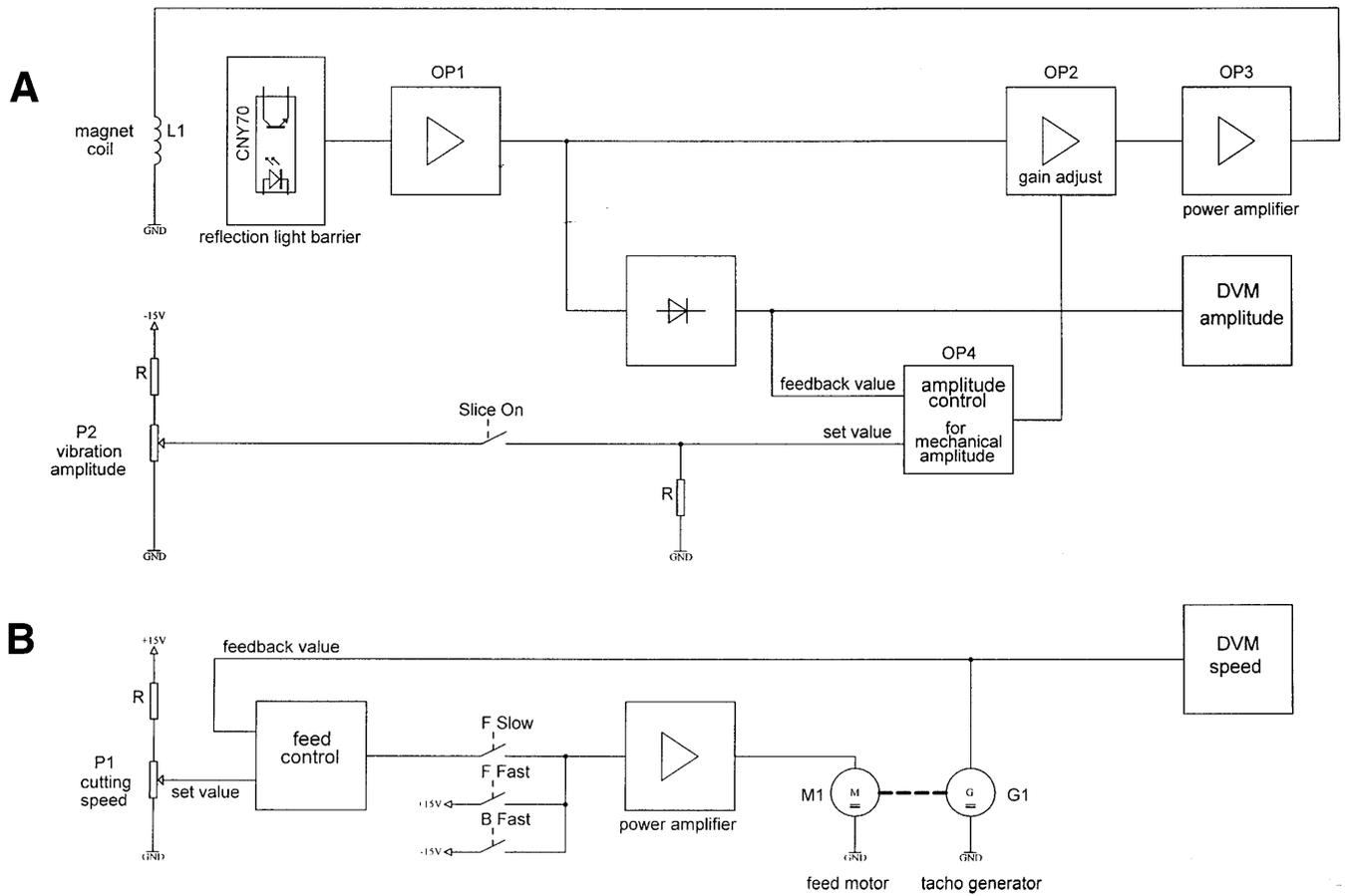
A

B

Fig. 2A, B Electronic circuit of the vibroslicer. **A** Circuit of the auto-resonant, mechano-electrical feedback system. The vibration is generated by the feedback loop established by operational amplifiers (*OP*s) 1–3. OP4 and 5 establish the automatic gain control. *DVM*, digital voltmeter. **B** Circuit for driving the DC motor with tacho-generator and gear, generating the slow horizontal movements of the probe holder. For details, see text

OP4 compares this signal with the set value from P2 and processes the difference signal with a proportional-integral element (time constant ≈1 s). The output of OP4 then controls the gain of OP2, leading to the generation of mechanical oscillations with constant amplitude, even during substantial changes of the mechanical load. When the head is at rest, the gain of OP2 is regulated initially to maximum (because its feedback input signal is zero, whereas the signal from P2 is different from zero). This initiates the vibration when the external switch is closed. The rectified output of OP1 is also displayed on a digital voltmeter (DVM amplitude) that indicates the horizontal oscillation amplitude after appropriate calibration.

Continuous horizontal probe holder movement

Cutting slices requires a slow and continuous horizontal relative movement between oscillating cutting blade and brain tissue. To generate this movement, the probe holder is clamped on a height-adjustable block mounted on a

Fig. 3 Photograph of the vibroslicer. A probe holder mounted on a height-adjustable block is visible in the *centre*. Height adjustment of the probe holder is made manually by means of the micrometer screw on the front (*left* in the figure). DC motor, tacho-generator and gear used for generating horizontal movement of the sample holder are situated within the main body, below the *folded cover*. The oblique panel on the *right* contains control and display elements. The block of stone (mass ≈40 kg) on which the vibroslicer is mounted is visible below the slicer

sliding table (Fig. 3). The entire system can be moved back and forth by a DC motor with a tacho-generator and gear (32 V; 6100 turns min⁻¹, gear 24:1; 35HNT2R-426SP204-R32 16 0 24; motor-tacho gear; API Portescap, La Chaux-de-Fonds, Switzerland). A feedback circuit controls the translation velocity independently of load (Fig. 2B); values between 0.08 mm min⁻¹ and 1.5 mm sec⁻¹ can be chosen as desired. The translation velocity is displayed on a digital voltmeter (DVM speed) after appropriate calibration.

Oscillation frequency

In the configuration described, the oscillation frequency is 93 Hz. In a first approximation, this frequency can be calculated as follows. The elasticity module (E) of this steel is 200 kN mm⁻² (according to steel data sheets). For a length l of 95 mm between fixation points and dynamic points, a thickness h of 2 mm and a width b of 40 mm, the spring constant D of a system of two parallel springs is:

$$D = \frac{2Ebh^3}{l^3} = 150\,N\,mm^{-1} \qquad (1)$$

(p. 269 in [11]). The total mass m of the permanent magnet blocks, the front piece and additional parts is ≈300 g. The resonance frequency (f) of this system can be estimated as:

$$f = \frac{1}{2\pi}\sqrt{\frac{D}{m}} = 112\,Hz \qquad (2)$$

(p. 632 in [11]). Predicted and measured resonance frequency are thus in approximate agreement; the deviation may be attributed to the additional mass contribution of the springs and the distributed nature of the mass. From Eqs. 1 and 2, it follows that the resonance frequency f is proportional to $l^{-3/2}$. This relation can be used to alter the oscillation frequency by changes in the free length of the leaf springs.

Real-time monitoring of vertical blade vibrations with a vibroprobe device

To measure vertical vibrations of the cutting blade of both the vibroslicer and commercial slicers in real time, we developed a "vibroprobe" device (Figs. 4 and 5). The principle of the operation is simple, based on a LED (emitter) and a photodiode (receiver; Fig. 4A). The mounted cutting blade shades part of the light beam between emitter and receiver, resulting in a change in the photodiode output signal. This output signal can be examined on an oscilloscope after amplification.

Construction details

As an emitter we used an infrared-light-emitting diode (LED SEP8736; Honeywell, Morristown, NJ, USA;
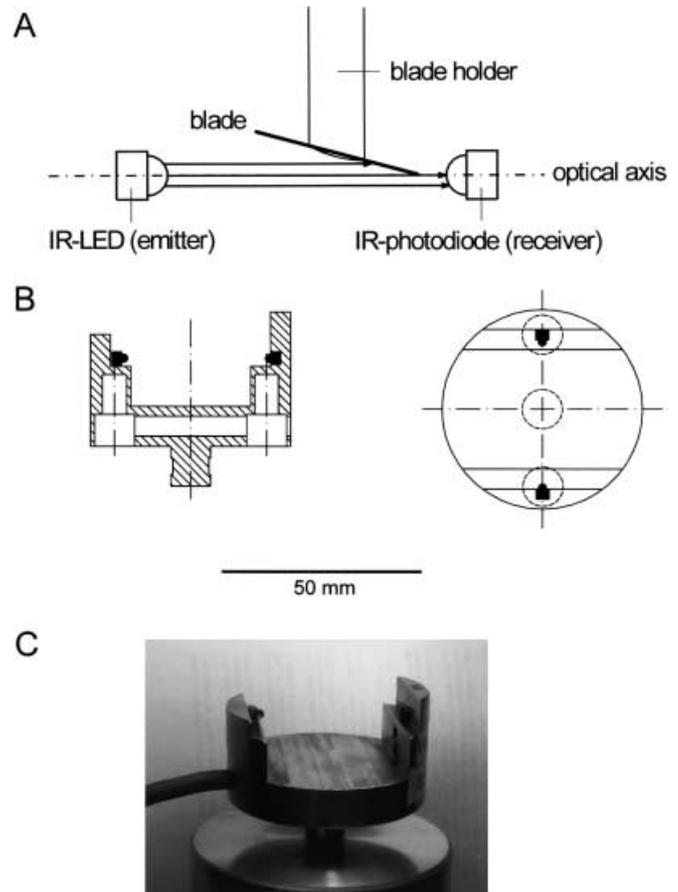

Fig. 4A–C Principle and assembly of the vibroprobe. **A** Principle of operation. The mounted cutting blade shades part of the light beam between emitter and receiver. Undesirable vibrations in the vertical direction (up and down) can be monitored by the variable shading of the light beam. **B** Schematic drawing of the body of the vibroprobe; view from side (*left*) and from top (*right*). *Filled structures* represent infrared-light-emitting diode (*IR-LED*) and photodiode. **C** Photograph of the vibroprobe before mounting on the slicer

maximal intensity at 880 nm; 10% intensity at 800 and 960 nm, respectively; 10° beam angle). As a receiver we used an infrared-sensitive photodiode (SFH229 FA; Infineon, Munich, Germany; maximal sensitivity at 900 nm; 10% sensitivity at 730 and 1100 nm, respectively; 17° acceptance angle). Emitter and receiver with infrared characteristics were chosen to minimize the effects of stray environmental light. Furthermore, emitters and receivers with near-point geometry were selected. The response time of the receiver is fast compared with the time course of mechanical events to be analysed; the measured 0–90% response time is ≈80 μs. Both emitter and receiver are mounted precisely on a horizontal axis, which allowed us to monitor selectively vertical blade movements.

A two-dimensional vibroprobe, with two emitter-receiver pairs mounted at right angles, may be also useful for measuring both vertical and horizontal vibrations and for making appropriate adjustments (not illustrated).
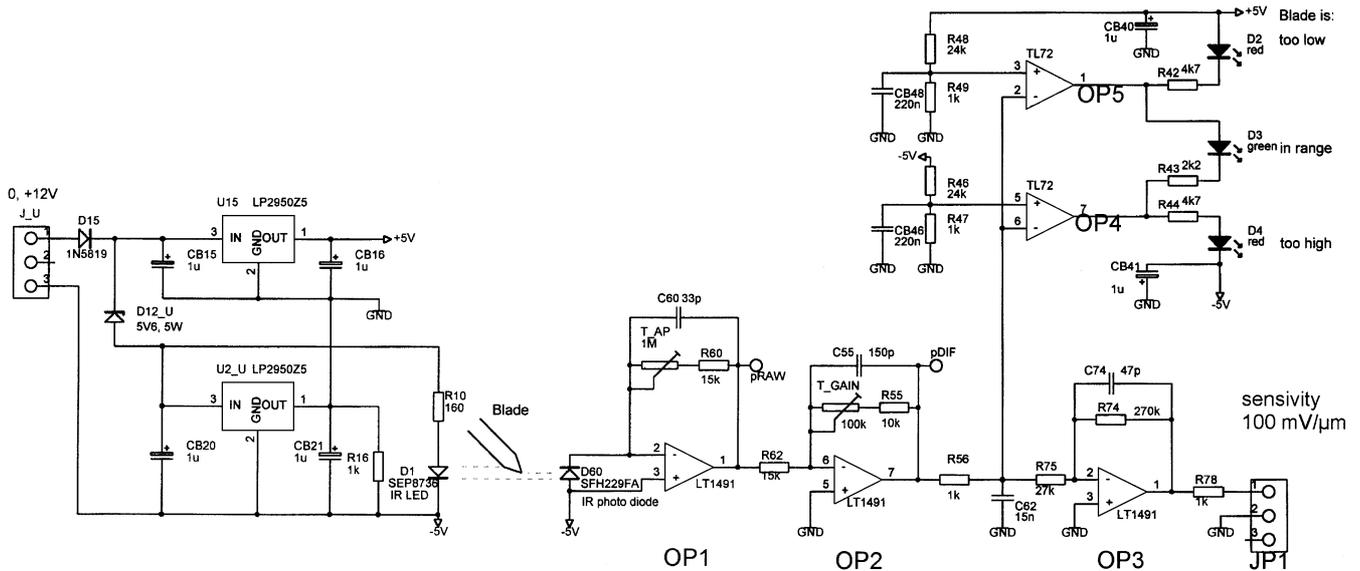
Use of the vibroprobe system

The vibroprobe device is mounted on the slicer instead of the probe holder. In the vertical (top-bottom) axis the cutting edge of the blade is positioned in centre of the light beam between emitter and receiver, the region in which the relation between position and electrical output signal is linear (Fig. 6C, inset). The output of the photodiode is amplified by three OPs (Fig. 5). If the cutting edge of the blade is positioned 2 mm from the receiver in the horizontal axis, the calibration factor is ≈100 mV μm^{-1}. To check the calibration factor, cutting blade and vibroprobe are shifted against each other by a defined distance.

Despite the use of infrared elements, stray environmental light may disturb vibroprobe measurements. Problems may be caused especially by nearby neon lights, since they induce artificial photodiode responses in the same frequency range as those generated mechanically. We therefore recommend that lights be dimmed before vibroprobe measurements. If this cannot be done, a two-photodiode assembly is proposed, in which the movement-related signal (illuminated photodiode) and the background signal (non-illuminated photodiode) are subtracted electronically.

Vibroprobe recording from different slicers

Figure 6A shows vibroprobe recordings from two commercial tissue slicers used in our lab (Campden 752 M, Campden Instruments, Loughborough, UK; Dosaka DTK-1000, Dosaka, Kyoto, Japan, both based on motor/ex-centre designs). In both cases, the amplitude of the horizontal oscillation is approximately 1 mm; that of the vertical vibration 3–20 μm (peak-to-peak amplitudes). However, vertical vibration differs not only between slicer types, but also between individual slicers of the same type, and even between the same slicers examined in different conditions at different times. Drifts in quality may be caused by mechanical wear, insufficient lubrication, insufficient cleaning, etc. Finally, vibroprobe monitoring also detects potential problems with both the slicer and the cutting blade (irregularities or bending). In case of doubt, exchanging the blade will help distinguish between these possibilities.

For comparison, Fig. 6B shows vibroprobe recordings from the vibroslicer after optimal adjustment (top trace) and during the adjustment procedure (bottom traces). When a horizontal oscillation amplitude is chosen that is comparable to that of the commercial slicers (1 mm), the amplitude of the vertical vibrations is much smaller than that of the commercial instruments.

A systematic analysis of the relation between the vertical and the horizontal oscillation amplitude of the cutting blade of the vibroslicer is illustrated in Fig. 6C. Vibroprobe recordings were made for ten different blades in the optimal position (determined as shown in Fig. 6A). For horizontal oscillation amplitudes of ≤3 mm, the vertical vibration amplitude is ≤1.5 μm. Thus, the oscillation generated by the vibroslicer is confined to a horizontal axis over a wide range of amplitudes.

Cutting slices with the optimized vibroslicer

Slicing procedures and solutions

To examine the quality of slices made with the vibroslicer, transverse hippocampal slices (300 μm thickness) were cut from the brains of 20- to 28-day-old rats. The

Fig. 6A–C Minimizing vertical vibrations with the vibroprobe. **A** Vibroprobe recordings for different slicers (slicer 1: Campden 752 M, slicer 2: Dosaka DTK-1000). Slicers 1 and 2 show a major component of vertical movement that has a frequency identical to the oscillation frequency ($\approx$40 Hz), indicating blade alignment problems. **B** Vibroprobe recording from a vibroslicer in the optimal position (*upper trace*) and during the adjustment procedure (*lower traces*; optimal position, one clockwise turn, and one counter-clockwise turn of the differential thread screw from the optimal position). Note that in **A** and **B**, the vertical vibrations have very different amplitudes (peak-to-peak $\approx$7 μm, 5 μm, and 0.5 μm, respectively), whereas the amplitudes of the horizontal oscillations were comparable (peak-to-peak $\approx$1 mm in all cases). **C** Peak-to-peak amplitude of vertical movement as a function of the horizontal oscillation for the adjusted vibroslicer. Measurements from the vibroslicer with ten different blades; measurements with the same blade are connected by *lines*. As individual cutting blades may differ from each other, an adjustment was made before every recording. *Inset*: vibroprobe calibration curve, i.e. output voltage at JP1 of the vibroprobe as a function of vertical position of the cutting blade
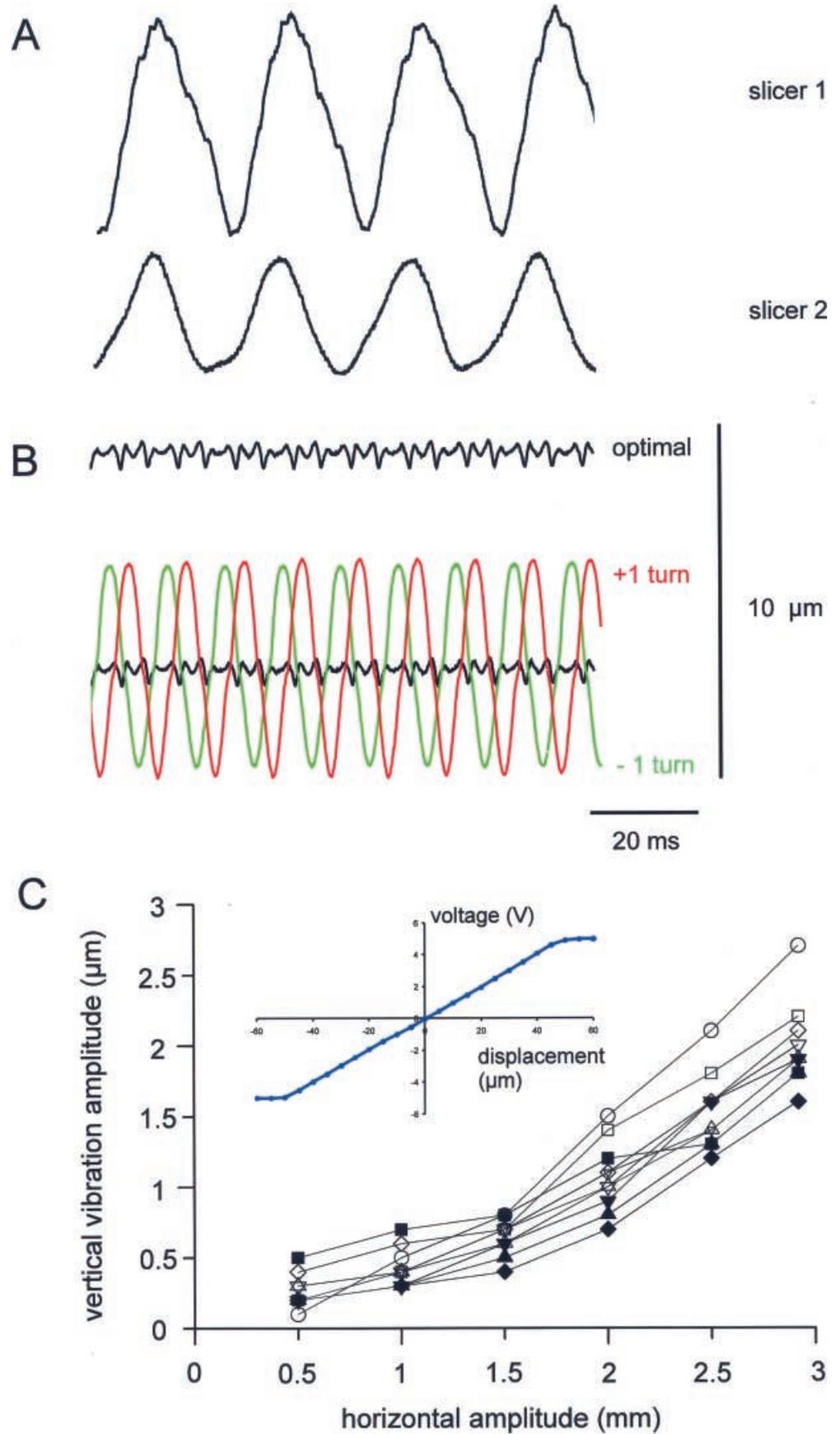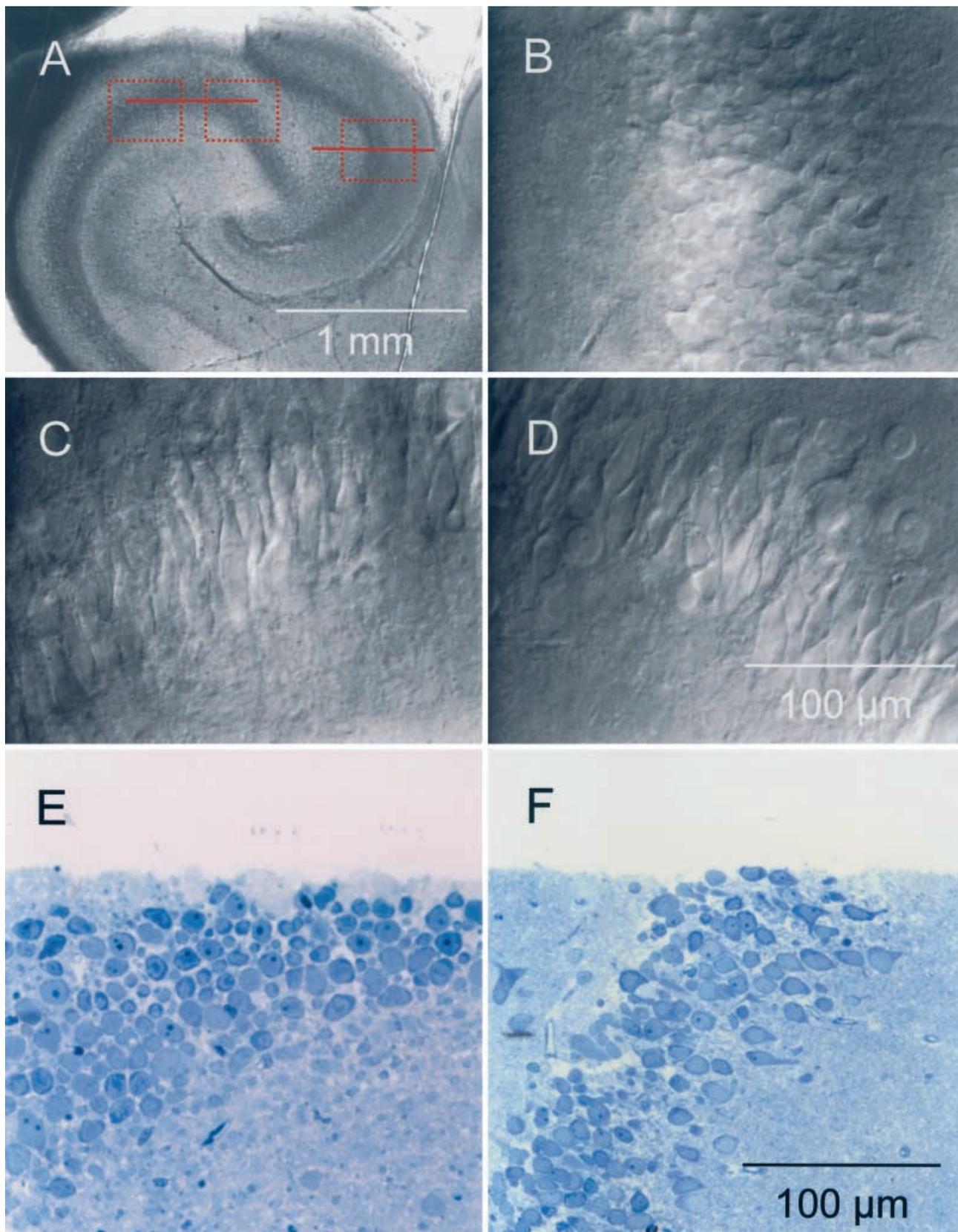
horizontal oscillation amplitude was set to 1.2–2.0 mm; the velocity of the probe holder to 4–10 mm min^{-1} (with an oscillation frequency of 93 Hz, this corresponds to a forward movement of 0.7–1.8 μm/cycle). The cutting blade was positioned at an angle of ≈15° to the horizontal plane. Slices were cut in ice-cold sucrose-containing physiological saline and transferred into a submerged-design maintenance chamber filled with sucrose-containing physiological saline at 35 °C for 30 min after cutting and at 22 °C during subsequent storage. Finally, slices were transferred into a recording chamber. For morphological analysis, sucrose-containing physiological saline was used for superfusion. For patch-clamp experiments, the sucrose-containing solution was replaced by sucrose-free solution at least 20 min before recording. The sucrose-containing physiological saline contained (in mM): 40 NaCl, 25 NaHCO$_3$, 10 glucose, 150 sucrose, 4.0 KCl, 1.25 NaH$_2$PO$_4$, 0.5 CaCl$_2$ and 7 MgCl$_2$ (≈350 mosmol/l). The sucrose-free physiological saline contained (in mM) 125 NaCl, 25 NaHCO$_3$, 25 glucose, 2.5 KCl, 1.25 NaH$_2$PO$_4$, 2 CaCl$_2$ and 1 MgCl$_2$. Both solutions were bubbled continuously with 95% O$_2$ / 5% CO$_2$.

Structural integrity of slices cut with the vibroslicer

To examine the preservation of cellular and subcellular elements in the superficial layers of the tissue, slices cut with the vibroslicer were processed for light and electron microscopy [7, 17]. Slices were fixed in 0.1 M phosphate buffer (PB) containing 1% paraformaldehyde and 1% glutaraldehyde (4 °C) and stored in the fixative overnight. Subsequently, slices were washed in PB and small blocks containing the regions of interest were dissected. The blocks were post-fixed in 1% osmium tetroxide, dehydrated in graded series of ethanol, transferred to propylene oxide, and embedded in Durcupan (Fluka, Buchs, Switzerland). Semi-thin sections were cut perpendicular to the plane of the slices, stained with toluidine blue and mounted under cover-slips using Eukitt (O. Kindler, Freiburg, Germany). Ultra-thin sections were cut in series with the semi-thin sections and analysed by electron microscopy using a Philips CM 100 electron microscope (Philips, Monza, Italy).

◄ **Fig. 7A–F** Light-microscopic analysis of slices cut by the vibroslicer. **A** Low-magnification infrared differential interference contrast (IR-DIC) image of a hippocampal slice (objective 5×, NA 0.12, A-Plan, Zeiss, Göttingen, Germany). Note grid threads (*left* and *right*). **B–D** High-magnification IR-DIC images of the dentate gyrus (**B**) and the hippocampal CA3 region (**C, D**) (objective 60×, NA 0.9, water immersion, LUMPlanFl/IR, Olympus, Tokyo, Japan). The focal plane was ≈10 μm below the surface of the slice. The approximate fields of view are indicated schematically by the *boxes* in **A**. Images in **A–D** were acquired using a frame grabber (Matrox Corona, Dorval, Canada) and a Pentium-PC. **E, F,** Light-microscopic analysis of semi-thin sections in the CA3 region (**E**) and the dentate gyrus (**F**). The approximate planes of the cut are indicated schematically by the *lines* in **A**. The *upper border* corresponds to the surface depicted in the IR-DIC images. All images were obtained from the same slice (prepared from a 21-day-old rat)

Figure 7 shows IR-DIC video-images [21] and light micrographs of the corresponding semi-thin sections of a hippocampal slice cut with the vibroslicer after optimization (see above). The IR-DIC images, taken with a focal plane ≈10 μm below the surface of the slice, illustrate that both superficial dentate gyrus granule cells (Fig. 7B) and CA3 pyramidal neurons (Fig. 7C, D) showed a high level of integrity. The light microscopic images of the semi-thin sections illustrate further that the majority of neurons appeared to be intact over the entire cross-section of the slice. As viable CA3 pyramidal neurons are difficult to obtain in hippocampal slice preparations, this provides a relatively stringent test of slice quality.

Figure 8 shows IR-DIC video-images and an electron micrograph of the stratum lucidum of a hippocampal slice, the region where mossy fibres terminate on CA3 pyramidal neurons. In Fig. 8A, IR-DIC video-images of a mossy fibre bouton (MFB) attached to the apical dendrite of a CA3 pyramidal neuron are depicted. Figure 8B shows a high-power electron micrograph of the stratum lucidum of a different slice. The MFB shown was located ≈10 μm below the surface of the slice. Note that the ultrastructure in these very superficial layers is remarkably well preserved.

Discussion

An ideal tissue slicer is able to generate large-amplitude and high-frequency oscillations in a horizontal axis, with minimal movements in the vertical axis. We constructed a slicer that fulfils these partly contradictory requirements. The vibroslicer head presented here includes several conceptionally novel features. First, a permanent-magnet-coil-leaf-spring system was used, which is very powerful and generates strictly horizontal forces. Second, the vibration is driven by an auto-resonant mechano-electrical feedback loop. This approach is greatly superior to systems that are driven below or above the resonance point, because the maximal oscillation amplitude is generated with the minimum external force. The approach is also superior to methods that first find, and then hold, the resonance frequency, because the resonance point changes during immersion of the cutting blade in solution. Third, an adjustment mechanism that allowed the cutting edge of the blade to be aligned with the major axis of the oscillation was employed.

To make this alignment as precisely as possible, we developed a vibroprobe device based on a LED-photodiode array that allowed vertical movements of the cutting blade to be monitored in real time. After optimization, the vibroslicer generates high-frequency (70–130 Hz, dependent on the length of the leaf springs used) and large-amplitude (up to 3 mm peak-to-peak) horizontal oscillations, while vertical vibrations of the blade are minimal, typically 0.5–2.0 μm or less after accurate adjustment. In addition to being essential for adjustment of the vibroslicer, the vibroprobe device is potentially useful for quantitative monitoring of the quality of commercial tissue slicers.

Fig. 8A–B Electron-microscopic analysis of the structural integrity of slices cut by the vibroslicer. **A** High-magnification IR-DIC images of the stratum lucidum, the region where the mossy fibres terminate (objective 60×, NA 0.9). A mossy fibre bouton (MFB, *circle*, diameter ≈4 µm) is visible close to the primary apical dendrite of a CA3 pyramidal neuron. *Left image* before, *right image* after approach with a patch pipette. *Inset* (*white trace*) shows a current-clamp recording of an action potential from the same MFB (1 ms pulse, 200 pA; *scale bars* 20 ms, 100 mV) (from [8], copyright by Cell Press). **B** High-power electron micrograph of the stratum lucidum from the slice shown in Fig. 7 (*b* MFB, *d* dendrite of a CA3 pyramidal neuron, *a* bundle of unmyelinated axons, presumably mossy fibre axons). Note the presence of desmosomes between bouton and adjacent dendrites. MFB shown in **B** was located ≈10 µm below the surface of the slice
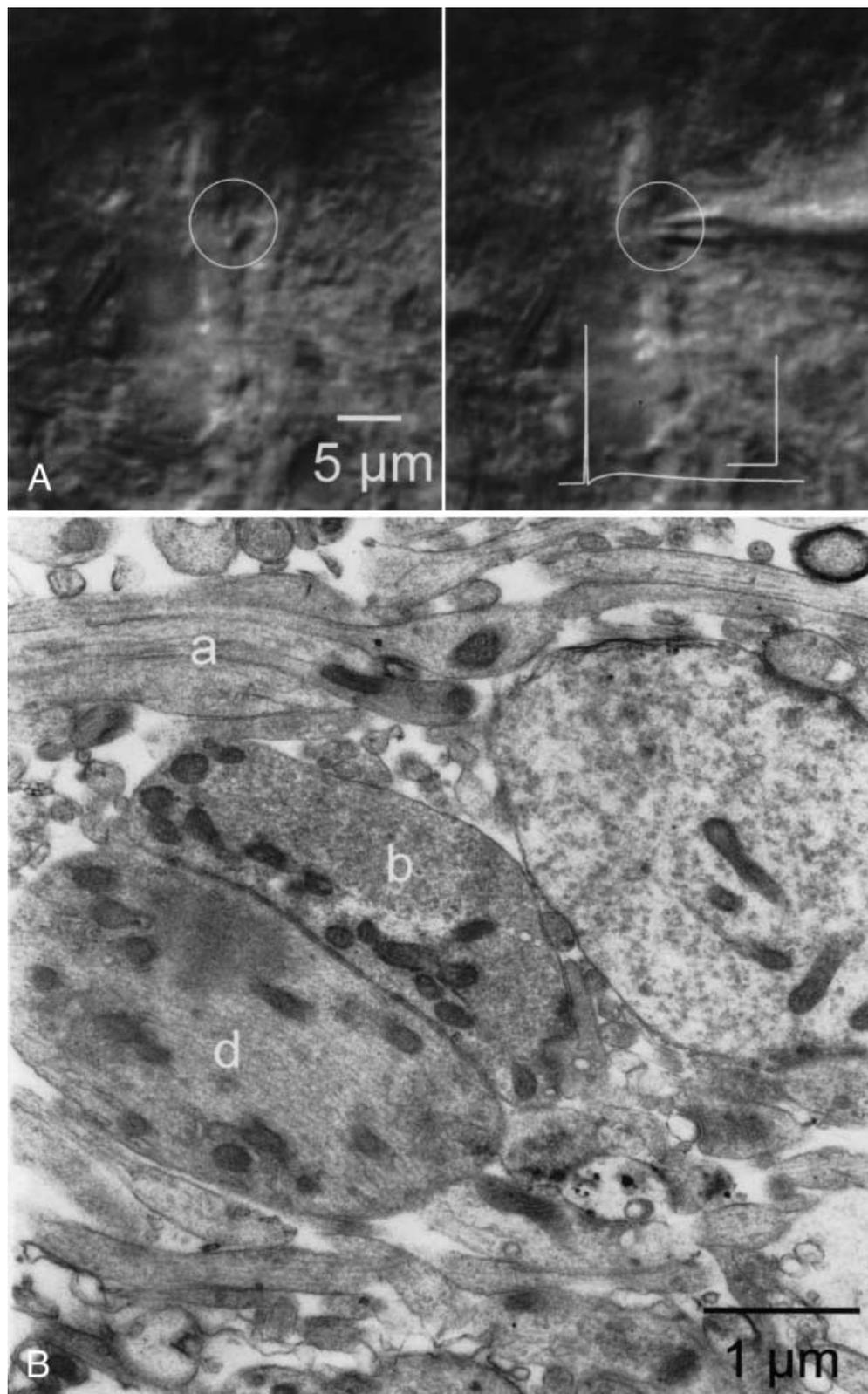
Provided that the biological problems of slicing, such as slow and inaccurate dissection, high bath temperature during cutting, poor conditions of the animal, etc. are eliminated, the use of vibroslicer and vibroprobe may lead to a significant improvement in slice quality. Using this novel technology, we were able to cut hippocampal slices with extremely well preserved surface layers. Light and electron microscopic analysis of slices cut with the vibroslicer indicated that cellular and subcellular elements were largely intact 10 µm below the surface (Figs. 7 and 8). In

contrast, slices cut with conventional methods often show a relatively small intact core region surrounded by relatively large debris zones on either side (e.g. [7, 17]). The potential value of this improvement is twofold. First, optimized slicing techniques will result in a better experimental yield and minimization of the artefacts of slice recording. Second, optimized slicing techniques will facilitate "difficult" experiments, such as paired recordings or recording from subcellular structures. A remarkable example is the direct patch-clamp recording from hippocampal MFBs in the slice [8], which has been facilitated substantially by the improvement of slicer technology.

References

1. Beitz W, Grote K-H (2001) Taschenbuch für den Maschinenbau, 20th edn. Springer, Berlin Heidelberg New York, p X6
2. Blanton MG, Lo Turco JJ, Kriegstein AR (1989) Whole cell recording from neurons in slices of reptilian and mammalian cerebral cortex. J Neurosci Methods 30:203–210
3. Borst JGG, Helmchen F, Sakmann B (1995) Pre- and postsynaptic whole-cell recordings in the medial nucleus of the trapezoid body of the rat. J Physiol (Lond) 489:825–840
4. Dodt H-U, Zieglgänsberger W (1990) Visualizing unstained neurons in living brain slices by infrared DIC-videomicroscopy. Brain Res 537:333–336
5. Edwards FA, Konnerth A, Sakmann B, Takahashi T (1989) A thin slice preparation for patch clamp recordings from neurones of the mammalian central nervous system. Pflügers Arch 414:600–612
6. Forsythe ID (1994) Direct patch recording from identified presynaptic terminals mediating glutamatergic EPSCs in the rat CNS, in vitro. J Physiol (Lond) 479:381–387
7. Frotscher M, Misgeld U, Nitsch C (1981) Ultrastructure of mossy fiber endings in in vitro hippocampal slices. Exp Brain Res 41:247–255
8. Geiger JRP, Jonas P (2000) Dynamic control of presynaptic Ca^{2+} inflow by fast-inactivating K^+ channels in hippocampal mossy fiber boutons. Neuron 28:927–939
9. Geiger JRP, Lübke J, Roth A, Frotscher M, Jonas P (1997) Submillisecond AMPA receptor-mediated signaling at a principal neuron-interneuron synapse. Neuron 18:1009–1023
10. Geiger JRP, Bischofberger J, Fröbe U, Pfitzinger S, Weber HJ, Haverkampf K, Jonas P (2001) Patch-clamp recording in brain slices with improved slicer technology (abstract). Pflügers Arch 441 (Suppl):R169
11. Hildebrand S (1983) Feinmechanische Bauelemente, 4th edn. Hanser, Munich
12. Kraushaar U, Jonas P (2000) Efficacy and stability of quantal GABA release at a hippocampal interneuron-principal neuron synapse. J Neurosci 20:5594–5607
13. MacVicar BA (1984) Infrared video microscopy to visualize neurons in the in vitro brain slice preparation. J Neurosci Methods 12:133–139
14. Markram H, Lübke J, Frotscher M, Roth A, Sakmann B (1997) Physiology and anatomy of synaptic connections between thick tufted pyramidal neurones in the developing rat neocortex. J Physiol (Lond) 500:409–440
15. Martina M, Vida I, Jonas P (2000) Distal initiation and active propagation of action potentials in interneuron dendrites. Science 287:295–300
16. Miles R, Poncer J-C (1996) Paired recordings from neurones. Curr Opin Neurobiol 6:387–394
17. Misgeld U, Frotscher M (1982) Dependence of the viability of neurons in hippocampal slices on oxygen supply. Brain Res Bull 8:95–100
18. Rice ME, Pérez-Pinzón MA, Lee EJK (1994) Ascorbic acid, but not glutathione, is taken up by brain slices and preserves cell morphology. J Neurophysiol 71:1591–1596
19. Sakmann B, Stuart G (1995) Patch-pipette recordings from the soma, dendrites, and axon of neurons in brain slices. In: Sakmann B, Neher E (eds) Single-channel recording, 2nd edn. Plenum, New York, pp 199–211
20. Schneggenburger R, Meyer AC, Neher E (1999) Released fraction and total size of a pool of immediately available transmitter quanta at a calyx synapse. Neuron 23:399–409
21. Stuart GJ, Dodt H-U, Sakmann B (1993) Patch-clamp recordings from the soma and dendrites of neurons in brain slices using infrared video microscopy. Pflügers Arch 423:511–518